

Conf-7205238-1

BNL-47765

DE92 019219

## Two-nucleon Production of Hyperons

### In an S=-1 Dibaryon Search

R. E. Chrien\*

Received by OST

Brookhaven National Laboratory, Upton N. Y. 11973

April 1992

### ABSTRACT

The double-charge-exchange reaction  $^3He(K^-, \pi^+)Xn$  was studied at  $p_{K^-} = 870$  MeV/c. In the missing mass range below the sigma-nucleon production threshold (3075 MeV/c<sup>2</sup>) events were detected and attributed to the two-nucleon reaction  $pp(K^-, \pi^+)\Lambda n$ . This reaction and mass range is supposed to be a fertile field for a search for the  $I = 1/2$ ,  $L = 1$  ( $^1P_1$ ) spin-singlet dibaryon suggested as the lowest mass  $S = -1$  dibaryon of bag model predictions. We find no need to invoke such an object to account for the observed events below  $\Sigma$  production threshold.

### I. INTRODUCTION

Bag models using phenomenology within the framework of quantum chromodynamics have successfully accounted for the experimentally known ground state mass spectra of the known hadrons - mesons and baryons[1]. Such models use a small number of adjustable parameters, such as the bag radius to fit the observed masses. These models are notable, however, for their predictions of a large number of objects not heretofore observed, including dibaryons, gluonium, and hybrid mesons. Those predictions have understandably stimulated many experimental searches for such objects.

REF ID: A2

DISTRIBUTION OF THIS DOCUMENT IS UNLIMITED

## **DISCLAIMER**

This report was prepared as an account of work sponsored by an agency of the United States Government. Neither the United States Government nor any agency thereof, nor any of their employees, makes any warranty, express or implied, or assumes any legal liability or responsibility for the accuracy, completeness, or usefulness of any information, apparatus, product, or process disclosed, or represents that its use would not infringe privately owned rights. Reference herein to any specific commercial product, process, or service by trade name, trademark, manufacturer, or otherwise does not necessarily constitute or imply its endorsement, recommendation, or favoring by the United States Government or any agency thereof. The views and opinions of authors expressed herein do not necessarily state or reflect those of the United States Government or any agency thereof.

Many searches have been reported in the non-strange sector ( $S=0$ ), and their results and interpretation lie outside the scope of this paper. We note in that passing, however, that one would expect non-strange dibaryons with masses exceeding the deuteron mass by at least the pion mass would be exceedingly broad and difficult to detect. On the other hand, the region of hyperons is much less researched, and it is conceivable that dibaryons with masses exceeding that of a hyperon-nucleon pair by less than a pion mass might be narrow and still have failed to be detected. Indeed, a number of dibaryon searches have been carried out and some claims of positive results reported.

At the present time several extensive searches for the so-called Jaffe H-particle (H for hexaquark) containing equal numbers of u, d, and s quarks in relative S-states are being carried out. The H is expected to be the most bound and most stable of the baryons; its mass is assumed to be less than that of two  $\Lambda$  hyperons, i.e., less than 2130 MeV/c<sup>2</sup>. The same bag model calculations, however, predict a pair of isospin 1/2 dibaryons with  $S = -1$ ; one spin triplet lying above the  $\Sigma$ -nucleon mass and one a spin singlet lying below the  $\Sigma$ -nuclear mass[2].

Aerts and Dover[3] have summarized the predicted differential cross sections for the production of the triplet dibaryons at various incident lab momenta for the reaction  $d(K^-, \pi^-)D_t$ . In the threshold region the  $\pi\Lambda$  and  $\pi\Sigma$  amplitudes interfere in the production of the  $\Sigma$  threshold cusp and this interference causes sizable uncertainties in the cusp shape and position, and hence uncertainties in the identification of a nearby presumed dibaryon. At higher mass values, the large quasifree production of  $\Sigma^0$  and  $\Sigma^+$  hyperons would tend to swamp the rather small  $D_t$  production, which Aerts and Dover predict to be at most only 2  $\mu b/sr$  at a scattering angle of 25°.

The  $D_s$  dibaryon search has a significant advantage over its triplet partner case. Since the  $D_s$  dibaryon is supposed to be below  $\Sigma$ -N threshold, the  $(K^-, \pi^+)$  reaction occurring on the proton pair in a  ${}^3\text{He}$  nucleus will produce the dibaryon free from

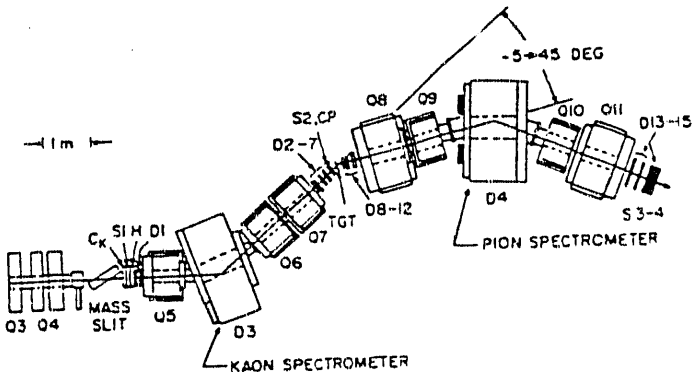


FIG. 1. The Moby Dick spectrometer at the end of the LESB-1 beam line at the BNL AGS.

competition from quasifree  $\Sigma$  production. Furthermore, the double-charge process will ensure that no first order  $\Lambda$  production will compete with  $D_s$  production. As pointed out in ref.[3], only the second order process  $pp(K^-, \pi^+) \Lambda n$  will yield hyperon  $\Lambda$  production below threshold, and clearly this reaction will be much less important than first-order production. The question of the size of such a reaction will be treated in the analysis section which follows.

## II. DESCRIPTION OF EXPERIMENT

The experiment was performed at the Brookhaven National Laboratory LESB-1 beam line at the Alternating Gradient Synchrotron and the Moby Dick hypernuclear spectrometer section. The spectrometer has been previously described in some detail[4], and the description of the analysis methods contained in ref. [4] applies, in the main, to the present studies, except where specifically noted. At the exit of the LESB-1 line, the kaon intensity was typically  $1-2 \times 10^5$  kaons/spill, with a 1.5 second spill occurring every 3 seconds. A typical ratio of unwanted particles (mostly pions and muons) to desired kaon was 7 to 1. Fig. 1 shows the downstream end of the

beam line and the Moby Dick spectrometer. Particle identification is afforded by time-of-flight involving the scintillators  $S_1$ ,  $S_T$ , and  $S_3$ , and by a Cerenkov counter  $C_K$  placed just downstream of the next slit. A lucite Cerenkov veto counter was used to veto decay pions placed just upstream of the target which would otherwise satisfy the time-of-flight condition for kaons.

The Moby Dick spectrometer was operated with a momentum acceptance of about 12 per cent and a solid angle acceptance of 15 msr. While the achievable resolution of Moby Dick is near 0.4 % for thin targets, for the extended liquid targets of the present experiment, an overall resolution of about 0.6% (5 MeV) was achieved.

The beam line and spectrometer were adjusted to central momenta of 870 MeV/c and 730 MeV/c for the kaon and pions, respectively. The momentum of 870 MeV/c was chosen to match a previous dibaryon search for the triplet dibaryon in the  $d(K^-, \pi^-)D_t$  reaction; there it was desired to minimize the  $I = 3/2$  production channels for the  $I = 1/2$  dibaryon, which decays to  $\Lambda p$ .

The  ${}^3\text{He}$  target consisted of a 25 cm long target vessel containing liquid  ${}^3\text{He}$  at a density of 0.075 gm/cm<sup>3</sup>. The target flask is 7.6 cm in diameter, and the target was placed so that rotated with the spectrometer. The targets were not centered in the beam; they were displaced about 3 cm to the left (viewing direction with the beam), so that the beam entering the target and scattered into the spectrometer did not interact with the target frame and walls. Fig. 2 shows a somewhat idealized view of the target geometry. Since the maximum dibaryon signal for the P-wave dibaryon occurs near 20°, the spectrometer was set to 20° for the major portion of this run. The total irradiation of the  ${}^3\text{He}$  target was about  $7.5 \times 10^{10}$   $\text{K}^-$  particles. In addition to the  $\pi^+$  runs, an experiment on the  ${}^3\text{He}(K^-, \pi^-)\Lambda pp$  reaction was run for a total of  $1.68 \times 10^9$   $\text{K}^-$  incident particles. The conditions of the run were identical to those for the  $(K^-, \pi^+)$  experiment with which it is directly compared.

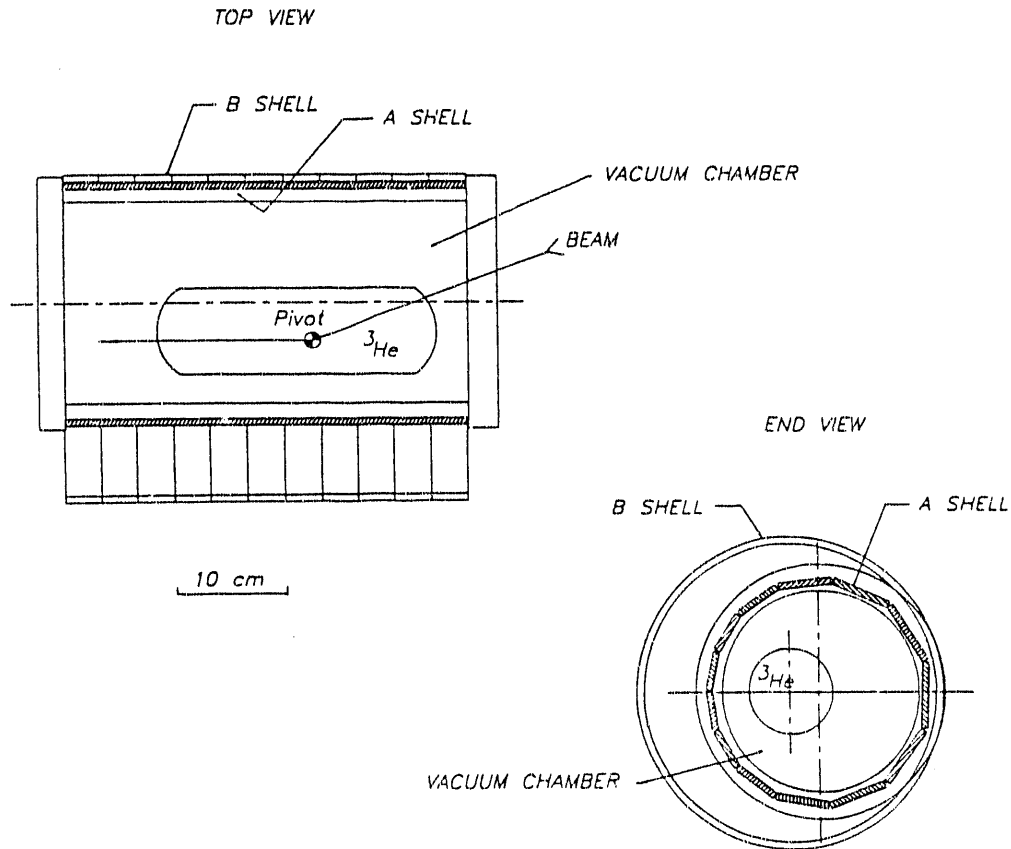


FIG. 2. A schematic drawing of the target region showing the placement of the A-shell (strip) and B-shell (ring) scintillators around the target.

Surrounding the target vessel was an array of scintillation counters. As shown in the figure, this array consisted of two layers: a) the A shell or inner layer consists of 13 strips arranged like barrel staves parallel to the pion beam axis, and b) the B-shell outer layer arranged a series of half-rings, 19 in number, joined together, and arranged like barrel hoops around the beam axis. As will be explained, these scintillators allow a crude characterization of the  $\theta$  (polar) and  $\phi$  (azimuthal) angles of emitted decay particles following reaction events in the  ${}^3\text{He}$  target. Because of the centerline displacement of the target as described in the previous paragraph,

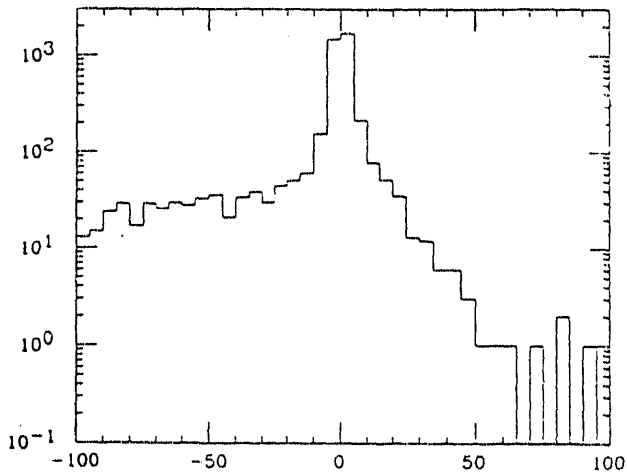


FIG. 3. The mass spectrum for the reaction  $^1\text{H}(K^-, \pi^+)\Sigma^-$  where the abscissa refers to the  $\Sigma^-$  kinetic energy.

the width of the A-shell strips was adjusted to provide nearly equal azimuthal angle increments around the target.

In addition to the  $^3\text{He}$  target, a liquid hydrogen target of density 0.07 gms/cm<sup>3</sup> was run for calibration purposes. These calibrations enabled us to evaluate (a) the charge-exchange background, as described below; (b) the cross section scale from the known  $p(K^-, \pi^+)\Sigma^-$  cross section (ref.[5]; and, (c) the system resolution from the  $\Sigma^-$  peak width. For the cross section calibration and resolution check runs the spectrometer was set to a central momentum of 670 MeV, placing the  $\Sigma^-$  peak at the center of the acceptance. The observed spectrum is displayed in figure 3.

Of special relevance in this figure is the appearance of background events below the  $\Sigma^-$  peak. These background events have their origin in the  $p(K^-, K^0)n$  single charge reaction. The subsequent two-pion decay ( $c\tau = 1.7$  cm) of the  $K^0$  component of that reaction takes place largely within the target volume. If one of the decay pions, the  $\pi^+$ , is emitted within the acceptance of the spectrometer, a  $(K^-, \pi^+)$  reaction is emulated. The observed background in fig. 3 is consistent with the  $(K^-, K^0)$  cross section data of Alston-Garnjost[6].

The reaction and charge-exchange processes were simulated by Monte Carlo techniques. Using the drift chamber and spectrometer information, one can project the incident kaon and exiting pion tracks back to a reaction vertex, localized to a distance of closest approach,  $T$ , which is a measure of the tracking accuracy. The distribution of this  $T$  variable is approximately exponential for a true reaction, with an rms value of about 4 mm, a value much smaller than the target diameter. For the background process, the  $T$  variable will tend to be larger because of the non-zero separation between the formation and decay points.

Using decay events recorded in the strip scintillators, and a reaction vertex as determined above, a "pseudo-reaction" angle  $\theta$  can be defined for the  $\pi^-$  from the  $K^0$  decay process, corresponding to its partner  $\pi^+$  accepted by the magnetic spectrometer. Because of the forward peaking of the charge-exchange processes, it was expected that the decay events would be characterized by relatively small pseudo-reaction angles, even though the "reaction" vertex, as described above, is not a well defined quantity. The observation suggests a way of cutting the phase space of the observed reactions to suppress the background event; small values of pseudotheta will represent  $K^0$  decays, while  $(K, \pi)$  reactions would be spread more uniformly in angle. This efficacy of this cut was suggested by Monte Carlo simulation and confirmed by experiment as described below.

Fig. 4 shows the invariant mass spectrum for the reaction  ${}^3He(K^-, \pi^+)Xn$ . The mass scale in this and succeeding figures is calculated assuming the recoil mass is a spectator neutron; hence the x-scale gives directly the presumed singlet dibaryon mass. The spectrometer was tuned to 730 MeV/c, a momentum expected for production of a dibaryon at 2100 MeV/c<sup>2</sup>, some 35 MeV/c<sup>2</sup> below the  $\Sigma$ -threshold. The figure also shows the spectrometer relative acceptance function and the positions of the  $\Lambda$ -N and  $\Sigma$ -N production thresholds. There is no requirement for a barrel coincidence in this figure.

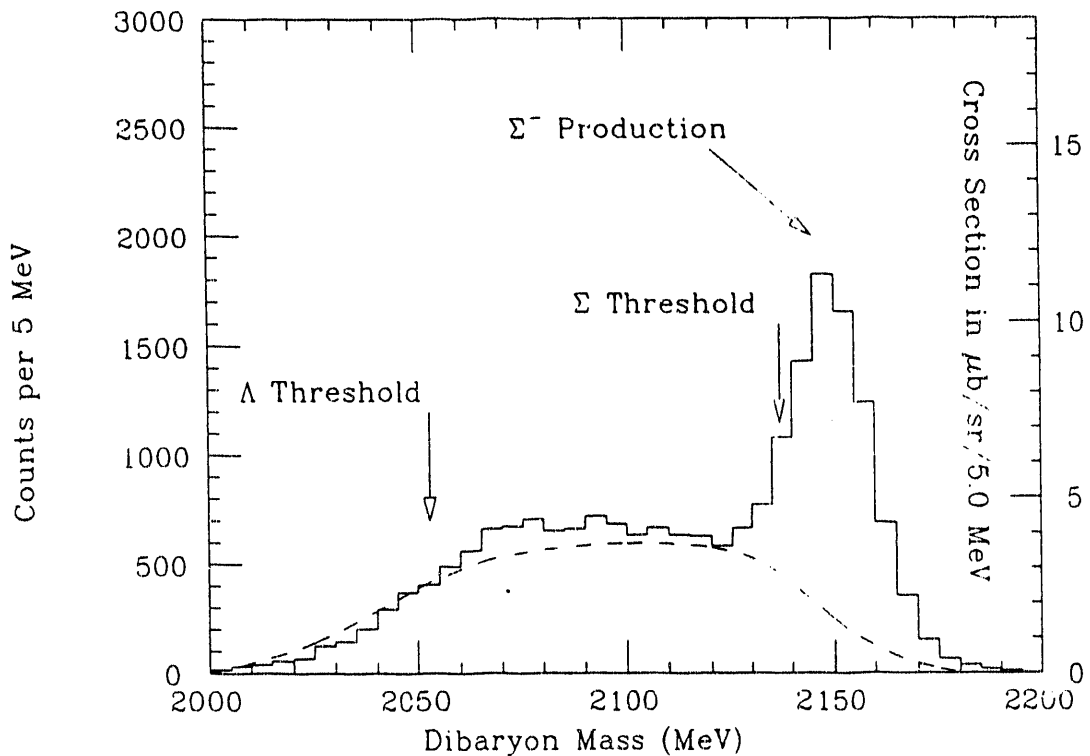


FIG. 4. The mass spectrum for the reaction  ${}^3\text{He}(K^-, \pi^+)nX$  at 870 MeV/c at  $\theta_{lab} = 20^\circ$ . The mass scale is calculated assuming the recoil mass consists of the dibaryon plus spectator neutron. The spectrum shown here is without imposing the requirement of observation of a decay pion in the barrel scintillators. Also shown, by the dashed curve, is the spectrometer relative momentum acceptance.

As indicated above, the region of interest for singlet dibaryon production lies between the  $\Lambda$  and  $\Sigma$  thresholds. The cross section scale on this and subsequent figures shown has been determined from the calibration against the data of Cameron et al [5] and the evaluation of the various cut efficiencies. It is apparent from this figure that a large background exists, at a level of  $0.8 \mu\text{b}/\text{sr}/\text{MeV}$ . The background shape, at low invariant mass, roughly follows the shape of the acceptance curve, implying that the mechanism responsible for it has a broad and relatively flat momentum

distribution over this acceptance range. The observed level of  $0.8 \mu\text{b}/\text{sr}/\text{MeV}$  is in accord with the expected production cross sections of Alston-Gjarnhorst et al[6]. We have no hesitation in attributing the bulk of these events to  $(K^-, K^0)$  charge-exchange reactions. There is no structure in this figure except for the large quasifree  $\Sigma^-$  production near  $2150 \text{ MeV}/c^2$ ; it is apparent that the  $\Sigma^-$  quasifree spectrum is cut off by the acceptance function at the high mass end.

It is instructive to examine the angular distributions of the decay pion events which are coincident with the  $(K^-, \pi^+)$  reaction trigger. As described previously, a reaction angle variable, called "pseudotheta" is defined by projecting the decay pion hit in the  $\theta$  and  $\phi$  scintillating strips back to an apparent vertex formed from the projection of the entrance and exit tracks. This pseudotheta variable is an approximation for a decay angle which ignores the non-zero  $K^0$  path length.

That this pseudotheta variable allows a rather effective separation between  $K^-, K^0$  charges and  $K^-$ -induced reactions is predicted by simulation and supported by experiment. Because of the relatively large forward peaking of the charge exchange cross section, it was expected that rejection of small angle events might provide good discrimination against this background. Fig. 5 shows a plot of event density in the plane defined by pseudotheta and excitation energy. This figure shows a marked difference between the pseudotheta distribution in the regions above and below  $\Sigma$ -nucleon thresholds; the region above  $\theta = 68^\circ$  clearly excludes the preponderance of  $(K^-, K^0)$  events and leaves a substantial fraction of the  $(K^-, \pi^+)$  reaction events as indicated by the  $\Sigma$ -N peak.

This conclusion also holds for an auxiliary  $(K^-, \pi^-)$  run[7] which was used to estimate the pseudotheta cut efficiency for dibaryon detection by invoking the assumption that the efficiency for dibaryon detection is the same as for  $\Lambda$  detection.

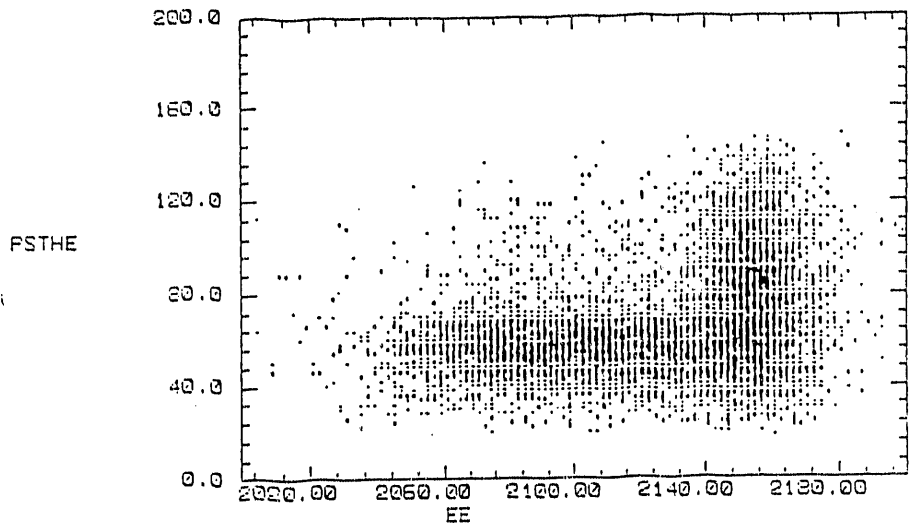


FIG. 5. The distribution of events in the plane defined by the variables pseudotheta and missing mass for the  ${}^3\text{He}(K^-, \pi^+)Xn$  reaction. Two distinct regions are seen in the figure; at the right is visible the quasi-free  $\Sigma^-$  production, and at the left is visible the charge exchange background. The plot illustrates the greater forward peaking for the charge exchange background reaction.

In this reaction, however, the  $K^0$  reaction is dwarfed by the large cross section for quasi-free  $\Lambda$ , so that a relatively pure sample of reaction events can be studied without the complication of the charge-exchange background. For all events in which a barrel hit of multiplicity 1 in the A or  $\phi$  shell and multiplicity 1 in the B or  $\theta$  shell is required, about 70% meet the pseudotheta  $\geq 68$  deg requirement. By contrast, a study of the pseudotheta distribution below the  $\Sigma$ -peak in the  $(K^-, \pi^+)$  spectrum of Fig. 4 shows that only 17 % of the events have pseudotheta angles in excess of 68 deg. Thus the application of a cut in pseudotheta to eliminate events below 68 deg improves the signal-to-noise ratio for dibaryon detection by a factor of 4 with only a modest loss in signal.

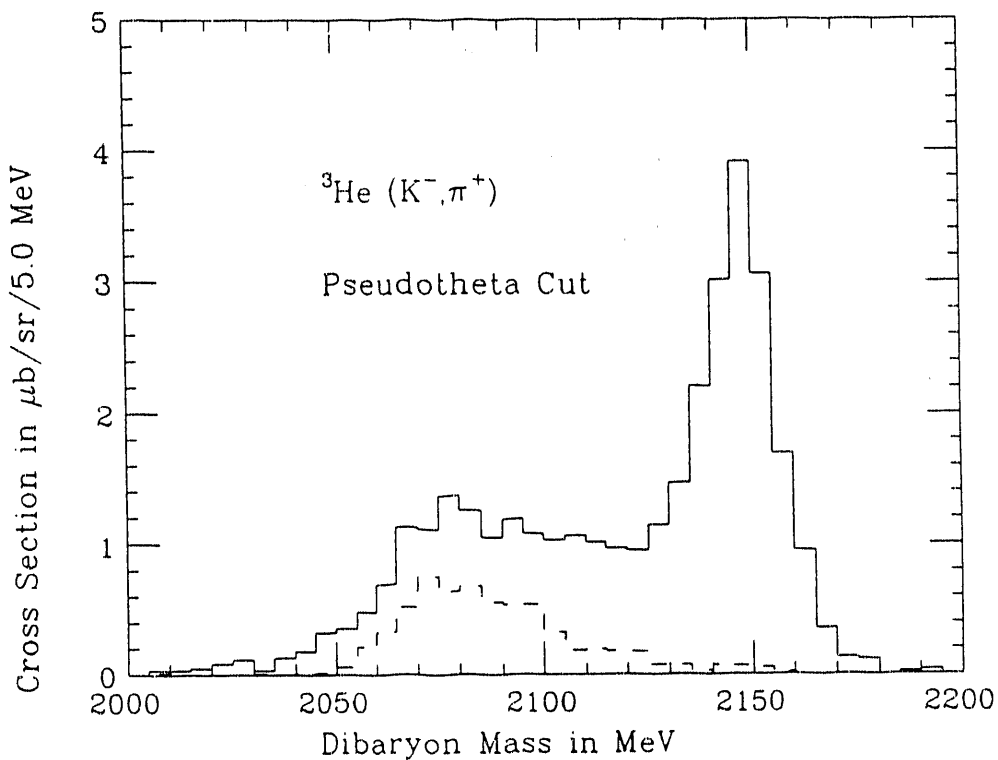


FIG. 6. The spectrum shown for  ${}^3\text{He}(K^-, \pi^+)Xn$  after suppression of the  $K^0$  background as described in the text. The normalized  $\Lambda$  production, determined from a separate experiment as discussed in the text, is shown as the dashed histogram.

In fig. 6 we show superimposed the spectrum remaining after the pseudotheta cut described above, for both  $(K^-, \pi^+)$  and  $(K^-, \pi^-)$  spectra. The relative normalization of these spectra will be discussed below. The shapes of the spectra suggest strongly that  $\Lambda$  production is responsible for a sizable fraction of the events lying below  $\Sigma$ -N threshold after application of the angle cut.

The two nucleon  $\Lambda$  production can take place coherently on two protons, as was pointed out by Aerts and Dover[3]. There are two alternative mechanisms:

- 1)  $p(K^-, K^0)n$ , followed by  $p(K^0, \pi^+)\Lambda$ , and

- 2)  $p(K^-, \pi^0)\Lambda$ , followed by  $p(\pi^0, \pi^+)n$

Although the interference between these processes complicates the calculation of the cross sections, the pion charge-exchange is known to be much larger than the kaon charge-exchange at this momentum[8]. Thus process 2) is dominant and has been estimated by Dover and Gal, using Glauber theory. The details of this calculation are given elsewhere[9]. The result of the calculation is that the two nucleon ( $K^-, \pi^+$ ) reaction leading to  $\Lambda$ 's is about 1 % of the ( $K^-, \pi^-$ ) single nucleon production of  $\Lambda$ 's on  $^3He$ .

The remaining events shown in Fig. 6 consist of a fraction (17 %) of the charge-exchange events which have evaded our pseudotheta cut, and a number of  $\Lambda$  events which are a result of virtual  $\Sigma$  production and rescattering (final state interaction) below the  $\Sigma$ -nucleon threshold. Karplus and Rodberg[10] use a complex scattering length expansion to describe the subthreshold  $\Lambda$  production in the ( $K^-, \pi^+$ ) reaction on deuterium. This approximation should be valid near threshold and is used here to account for the rapidly-rising event rate near 2135 MeV/c<sup>2</sup>. It has been shown by Dalitz[11] to give a reasonable representation of the cusp region. In applying the Karplus and Rodberg formalization, we have ignored the spectator neutron.

The complex scattering length expansion leads to the relations,

$$\tan \delta_{\Sigma}^{(0)} = -k_{\Sigma}(a_0 - i\eta_0),$$

$$|f_{\Sigma\Lambda}^{(0)}|^2 = \frac{\kappa_{\Sigma}\eta_0}{(1 - \kappa_{\Sigma}a_0)^2 + (\kappa_{\Sigma}\eta_0)^2};$$

and

$$k_{\Sigma} = i\kappa_{\Sigma} \text{ below threshold,}$$

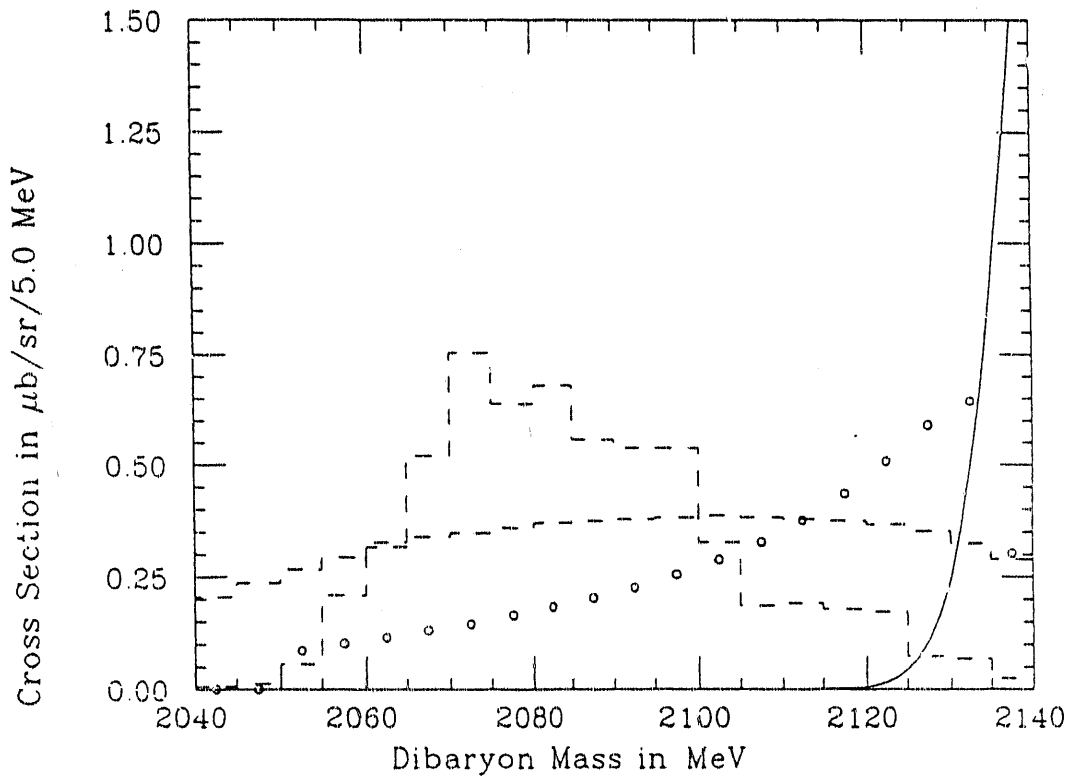


FIG. 7. The three background components and the  $\Sigma$  quasi-free components making up the spectrum of the previous figure are shown separately here.

where  $k_\Sigma$  represents the relative momentum between the recoiling  $\Sigma^0$  and proton. Values of  $\eta_0$  and  $a_0$  of about 0.003 ( $\text{MeV}/c^{-1}$ ) fit the tail region fairly well, although the data do not determine these values very accurately. The sum of the three background components discussed above are fit to the data of fig. 6 using a least-squares criterion to determine the relative fractions of each component. The magnitudes of the three components and the contribution of the quasi-free  $\Sigma$  component (modified by the spectrometer acceptance function) are shown in fig. 7.

### III. DISCUSSION OF RESULTS

After the calculation of the subthreshold contributions described above, the difference between the fitted and observed spectrum is shown in Fig. 8 as "net counts," along with the  $\pm$  one sigma error band limits of  $0.18 \mu\text{b}/\text{sr}/\text{MeV}$ . Recalling that the putative dibaryon would be Fermi-broadened over an interval of  $25.0 \text{ MeV}$ , we estimate the sensitivity of the experiment as approximately  $0.5 \mu\text{b}/\text{sr}$  from the rms fluctuations appearing in this net spectrum. Thus a dibaryon of  $0.5 \mu\text{b}/\text{sr}$  would not be visible in our data, while a  $2.0 \mu\text{b}/\text{sr}$  dibaryon could be seen with a confidence level of 4.0 sigma.

The observation of a dibaryon has been claimed by H. Piekacz[12] for data obtained from the  $(K^-, \pi^-)$  reaction on  ${}^2\text{H}$  at a mass of  $2144 \text{ MeV}/c^2$ . This dibaryon has been identified with the p-wave strangeness = -1 dibaryon  $D_t$  of the bag model. Piekacz assigns a cross section of  $25.6 \mu\text{b}/\text{sr}$  to that resonance. This value is far larger than the prediction of  $2 \mu\text{b}/\text{sr}$  of Aerts and Dover[3]. Putting aside this discrepancy, one might wish to associate some events below  $\Sigma$  threshold as the spin singlet partner  $D_s$  for the presumed dibaryon. Aerts and Dover calculate a ratio of four between the dibaryons  $D_t$  and  $D_s$  produced by the  $(K^-, \pi^-)$  and  $(K^-, \pi^+)$  reactions respectively.

In Fig. 8 we show the expected size of the broadened dibaryon  $D_s$  partner, based on the calculated ratio from Aerts and Dover. The position of the dibaryon is arbitrarily chosen to match the largest fluctuation in the net spectrum. It is apparent that we can rule out a dibaryon of that size from our data. There is no way to reconcile the present  ${}^3\text{He}$  results and the reported  ${}^2\text{H}$  dibaryon claim within the same bag model calculation.

While we cannot, from these data, rule out a dibaryon of the size predicted by Aerts and Dover -  $0.5 \mu\text{b}/\text{sr}$ , there is no need to introduce some unconventional

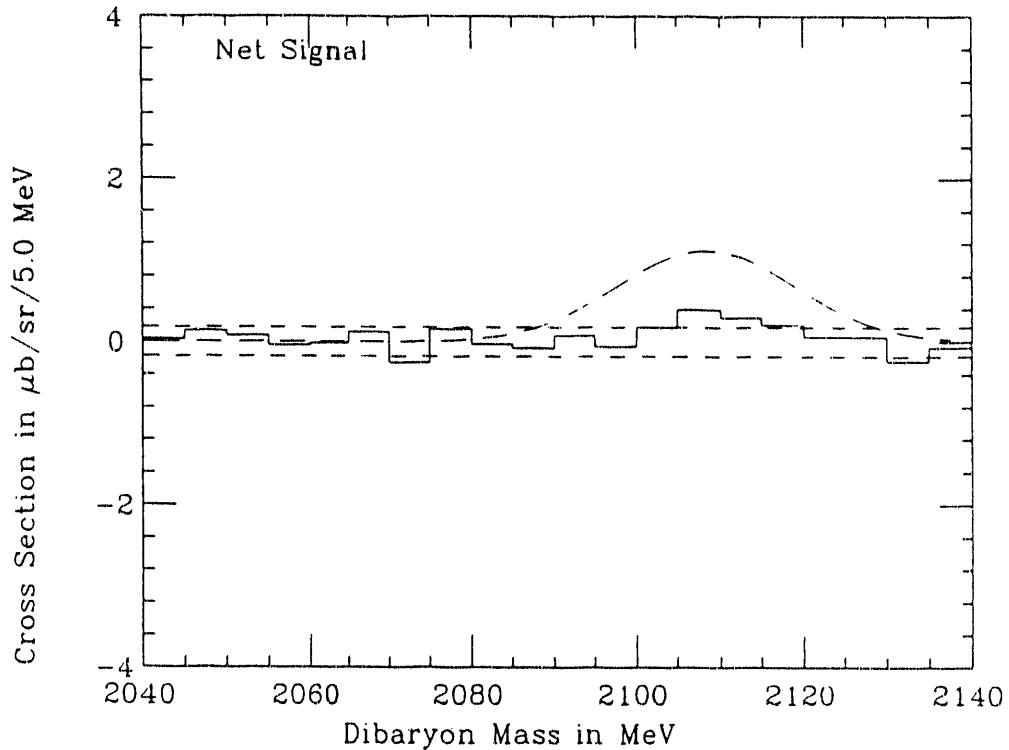


FIG. 8. The net signal in the missing mass region between  $\Lambda$  and  $\Sigma$  thresholds after all three background subtractions: a) the 2-step  $\Lambda$  production, b) the subthreshold  $\Sigma$  production and subsequent  $\Sigma - \Lambda$  conversion, and c) the residual  $K^0$  background not removed by the pseudotheta cut. The indicated error bands correspond to  $\pm 0.18 \mu\text{b}/\text{sr}$  and are 1 sigma limits. The curve shown represents the dibaryon signal for  $D_t$ , consistent with the reported  $D_t$  signal of ref.[12]. That dibaryon size is clearly ruled out by this experiment.

mechanism to account for events below the  $\Sigma$  threshold. They are due either to 1)  $K^-, K^0$  charge-exchange, 2)  $(K^-, \pi^+)$  production of  $\Lambda n$  from 2-nucleons, or 3) subthreshold  $\Sigma$  production and subsequent  $\Sigma - \Lambda$  conversion.

#### IV. SUMMARY

Events below the  $\Sigma$  production threshold which result from  $(K^-, \pi^+)$  interactions on  ${}^3\text{He}$  can result from second-order processes involving two nucleons. We have shown that after removing the very substantial  $(K^-, K^0)$  charge-exchange reaction which can mimic reaction events, two types of second-order processes account for  $\Lambda$  events. One is due to  ${}^3\text{He}(K^-, \pi^+)\Lambda n$  reaction which can be mediated by coherent strangeness and charge-exchange reactions. The cross section for this process has been determined from experiment to be about 1 % of the analogous  $(K^-, \pi^-)$  reaction; it accounts for much of the data below an invariant mass of 2100 MeV/c<sup>2</sup>. The remainder of the observed events is due to virtual  $\Sigma$  production and subsequent  $\Sigma - \Lambda$  conversion, which becomes the dominant  $\Lambda$  production process near  $\Sigma$  threshold. At a level of about 1  $\mu\text{b}/\text{sr}$  there is no need to invoke any other mechanism, in particular, the production of a strange dibaryon.

It is instructive to compare the search for dibaryons in deuterium and in  ${}^3\text{He}$ . In the former case the  $D_s$  dibaryon is accompanied by first-order  $\Lambda$  and  $\Sigma$  quasifree production and the problem is separating the dibaryon from a large underlying background. In the latter case, the  $D_s$  dibaryon search is conducted amidst a much smaller background but is affected by the momentum broadening associated with the unobserved spectator background. Clearly both experiments are required to establish the presence of those dibaryons. The present level of sensitivity is not adequate to rule out dibaryons at a level of less than 1  $\mu\text{b}$  but, as demonstrated here, it is clearly adequate to rule out dibaryons produced at levels of more than 1  $\mu\text{b}/\text{sr}$  in  ${}^3\text{He}$  and 4  $\mu\text{b}/\text{sr}$  in deuterium. More definitive limits would require experiments with better statistics.

#### V. ACKNOWLEDGEMENTS

The author acknowledges many valuable discussions with the collaborators of E820, as well as conversations with Reyad Sawafta, Carl Dover, and Avraham Gal.

## REFERENCES

- Representing the E820 Collaboration: K. Johnston, E.V. Hungerford, T. Kishimoto, B.W. Mayes, L.G. Tang, S. Bart, R.E. Chrien, L. Lee, P.H. Pile, R. Sutter, K. Hicks, T. Fukuda, R. Krauss, D.R. Gill, R. Stearns, and H. Seyfarth
- [1] A. W. Thomas, *Adv. Nucl. Phys.* **13**, 1 (1984),
- [2] P. J. G. Mulders, *et al.* *Phys. Rev.* **D25**, 1269; **D26**, 3035 (1982)
- [3] A. T. M. Aerts and C. B. Dover, *Nucl. Phys.* **B253**, 116 (1985).
- [4] R. E. Chrien *et al.*, *Phys. Rev.* **C41**, 1062 (1990)
- [5] W. Cameron *et al.*, *Nucl. Phys.* **B193**, 21, (1981)
- [6] M. Alston-Garnjost *et al.*, *Phys. Rev.* **D17**, 2216 (1978)
- [7] T. Kishimoto, spokesman, AGS Experiment 829
- [8] R. A. Arndt and L. D. Roper, SAID (Scattering Analysis Interactive Dial-in), VPI, unpublished, (1991); R. A. Arndt *et al.* *Phys. Rev.* **D28**, 97, (1983)
- [9] This calculation is to be published in a paper submitted to a memorial issue of the Czechoslovak Journal of Physics in honor of Jan Zofka by R. E. Chrien, C. B. Dover, and A. Gal. This calculation employs methodology described by C. B. Dover, *Nukleonika* **25**, 521 (1980), but corrects an error appearing therein.
- [10] R. Karplus and L. Rodberg, *Phys. Rev.* **115**, 1058 (1959).
- [11] R. H. Dalitz, *Nucl. Phys.* **A354**, 101c (1981)
- [12] H. Piekarsz, *Nucl. Phys.* **A479**, 263c, (1988); see also H. Piekarsz, in *AIP Conference Proc.* **243**, 576 (Conference on Intersections between Nuclear and High Energy Physics, Tucson, Arizona) (1991)

Research has been performed under contract No. DE-AC02-76CH00016 with the United States Department of Energy.

END

DATE  
FILMED  
9/28/92

